

The luminosity dependence of the Type 1 AGN fraction

Chris Simpson^{*}

Department of Physics, University of Durham, South Road, Durham DH1 3LE

28 July 2021

ABSTRACT

Using a complete, magnitude-limited sample of active galaxies from the Sloan Digital Sky Survey (SDSS) we show that the fraction of broad-line (Type 1) active galactic nuclei increases with luminosity of the isotropically-emitted [O III] narrow emission line. Our results are quantitatively in agreement with, and far less uncertain than, similar trends found from studies of X-ray and radio-selected active galaxies. While the correlation between broad-line fraction and luminosity is qualitatively consistent with the receding torus model, its slope is shallower and we therefore propose a modification to this model where the height of the torus increases slowly with AGN luminosity. We demonstrate that the faint-end slope of the AGN luminosity function steepens significantly when a correction for ‘missing’ Type 2 objects is made and that this can substantially affect the overall AGN luminosity density extrapolated from samples of more luminous objects.

Key words: galaxies:active – galaxies: Seyfert

1 INTRODUCTION

Active galactic nuclei (AGNs) were once thought to be a rare phenomenon whose major cosmological impact was in their ability to be seen out to great distances. However, the discovery of super-massive black holes in the centres of nearby galaxies has led to the view that all galaxies went through an active phase. Furthermore, calculations have shown that the energy produced during this phase is sufficient to drive material out of the host galaxy (Silk & Rees 1998; Fabian 1999). Feedback such as this can explain the tightness of the correlation between the masses of the black hole and host galaxy bulge (e.g., McLure & Dunlop 2002), and it has been suggested that such a process may perform a key role in shaping the galaxy luminosity function (Benson et al. 2003).

Semi-analytic models of galaxy formation (e.g., GALFORM; Cole et al. 2000) are now being adapted to investigate the role of AGN-driven feedback, and determine whether a self-consistent picture of both AGN and galaxy formation and evolution can be developed. It is to be hoped that progress in this field may provide important insights into some of the major outstanding issues in AGN research and, in particular, the question of AGN triggering. Early attempts at this (e.g., Kauffmann & Haehnelt 2000) have appeared encouraging in their ability to fit both the galaxy and QSO luminosity functions but, by failing to make the distinction between the QSO and AGN luminosity functions, they fail to account for the possibly significant population of “Type 2 QSOs” which have been postulated to explain the shape of the Cosmic X-ray Background (CXB; e.g., Comastri et al. 1995).

The cosmological importance of these objects is only exceeded by their elusiveness, since their optical continua closely

resemble those of normal galaxies and therefore they cannot be identified by the colour-selection techniques used for QSOs (e.g., Schmidt & Green 1983). Radio selection has allowed the radio-loud population of Type 2 QSOs (i.e., radio galaxies) to be identified, but radio sources comprise only a small fraction of the total AGN population. Hard X-ray selection has failed to locate the luminous narrow-line AGN in the numbers predicted by model fits to the CXB but current X-ray telescopes are unable to find distant AGN with Compton-thick absorption, and such objects are known to exist in abundance locally (e.g., Risaliti, Maiolino & Salvati 1999). Large spectroscopic surveys such as the Sloan Digital Sky Survey (SDSS; York et al. 2000) make it possible to identify AGN in an unbiased manner and therefore determine for the first time the fraction of Type 2 AGN.

In the simple unified model for AGN, Type 1 and Type 2 objects (i.e., those which display broad permitted lines, and those which show narrow lines only, respectively) differ only in terms of the angle which the observer’s line of sight makes with the axis of a dusty torus (see Antonucci 1993 for more details). If this angle is larger than some critical angle, θ_c , the line of sight to the central regions (which includes the broad line region) is blocked by the torus and a Type 2 AGN is seen. QSOs are therefore only a subset of the AGN population and no cosmological distinction should be made. If θ_c has no dependence on luminosity, then the QSO and AGN luminosity functions differ only in terms of their space density normalization.

However, the almost identical SEDs of QSOs just longward of $1\,\mu\text{m}$ (e.g., Kobayashi et al. 1993; Elvis et al. 1994) imply that the location of the inner wall of the torus is set by the distance from the nucleus at which dust reaches its sublimation temperature. This idea is supported by the observed time delays between variations in the optical and near-infrared continua (e.g., Fairall 9; Clavel,

^{*} Email: Chris.Simpson@durham.ac.uk

Wamsteker & Glass 1989). In more luminous objects this distance is further away and, if the height of the torus remains constant, the critical angle θ_c must increase, thereby leading to a luminosity dependence in the observed Type 1 AGN fraction. This is known as the ‘receding torus’ model and was first suggested by Lawrence (1991).

Of course, the height of the torus need not be the same in all objects but, since the luminosity dependence of its inner radius is the result of basic physics, it would be even more surprising if its height varied in such a way as to produce a constant opening angle. A variation in the Type 1 AGN fraction with luminosity is therefore to be expected, although the size of any such variation may be small. If it is large, however, then direct comparisons between the AGN luminosity function produced by models and the QSO luminosity function derived from observations (such as that undertaken by Kauffmann & Haehnelt 2000) are seriously compromised.

A number of authors have investigated possible evidence for the receding torus model, frequently using radio-selected AGN samples which are unbiased in terms of spectral type. These studies (e.g., Hill, Goodrich & DePoy 1996; Simpson, Rawlings & Lacy 1999; Willott et al. 2000; Simpson & Rawlings 2000; Grimes, Rawlings & Willott 2004) have all supported the receding torus model, while Simpson (1998) showed how it could explain apparent differences in supposedly isotropic properties between radio galaxies and radio-loud quasars with the same radio luminosity. Recent deep hard X-ray surveys have enabled similar analyses to be performed on samples of radio-quiet AGN, and the same trend is seen (Ueda et al. 2003; Hasinger 2004).

The case for the receding torus model appears strong, although most of the samples studies so far are relatively small. Alternative models for unification exist and include warped obscuring discs, broken shells of material, or an evolutionary scenario where the black hole is at first smothered but powers a wind which is eventually able to blow away material and allow the QSO to be directly observed. However, even if the receding torus model is incorrect, the number of Type 2 AGN need to be determined in order for AGN to fulfill their cosmological potential. In this paper, we construct separate [O III] emission line luminosity functions for broad and narrow-line AGN from the Second Data Release (DR2) of the SDSS which we use to investigate how the broad-line fraction varies with luminosity. The format of the paper is as follows. In Section 2 we describe how we have produced a sample of emission-line galaxies from the SDSS DR2 catalogue, and in Section 3 we describe the steps taken to produce luminosity functions for both Type 1 and Type 2 AGN. In Section 4 we derive the Type 1 AGN fraction and discuss the implications of our findings. Finally in Section 5 we present a summary. Throughout this paper we adopt a flat cosmology with $\Omega_m = 1 - \Omega_\Lambda = 0.3$ and $H_0 = 70 \text{ km s}^{-1} \text{ Mpc}^{-1}$.

2 SAMPLE SELECTION

The SDSS DR2 spectroscopic catalogue covers 2627 deg^2 down to a Petrosian magnitude of $r' < 17.77$ (in addition to colour-selected QSO candidates which we exclude by means of this magnitude cut). Spectra are taken through 3-arcsecond diameter fibres, and so we must impose distance (i.e., redshift) limits on our sample. The fibres will not encompass the entire emission line region for nearby AGN, since this can be $\sim 1 \text{ kpc}$ in size (e.g., Wilson & Tsvetanov 1994), while the dilution by starlight in distant galaxies will make the detection of emission lines more difficult. Kauffmann

et al. (2004) show that a Seyfert 2 sample with a luminosity limit $L_{[\text{O III}]} > 10^7 L_\odot$ and redshift limits $0.02 < z < 0.30$ does not suffer from aperture biases, and we therefore adopt the same constraints for our sample. This produces a catalogue of 4304 objects.

We do not apply any reddening corrections to the line luminosities. This is partly for practical reasons, since there is no reliable way to determine the reddening to the narrow-line region in broad-line objects. This is always a problem for studies which aim to compare the emission line properties of Type 1 and Type 2 AGN, although the fact that [O III] emission is seen to be isotropic when no reddening correction is applied (Mulchaey et al. 1994) suggests that differences between the mean reddening to the two types of galaxy must be small. Dahari & De Robertis (1988) estimate that the median difference is $E(B - V) \approx 0.2$, corresponding to a factor of ~ 1.7 at 5007 \AA . We will address whether this could have an impact on our results later.

We also do not correct our emission line fluxes for underlying stellar absorption. Since all our galaxies have very luminous [O III] emission lines, they will also have luminous $\text{H}\beta$ emission which is expected to dominate over any absorption. Wake et al. (2004) find that the observed AGN fraction is not sensitive to whether this correction is made.

3 ANALYSIS

3.1 Spectral classification

The SDSS spectroscopic pipeline produces a classification for all objects, based on principal component analysis (Schlegel et al., in preparation). For our sample of objects, this classification is either ‘‘QSO’’ (890 objects) or ‘‘galaxy’’ (3414 objects), which might be expected to correspond to AGN Types 1 and 2, respectively. However, while all objects classified as QSOs are expected to display broad emission lines, the galaxy classification will include starburst galaxies as well as objects classified as Type 1.8 or 1.9 (where broad $\text{H}\alpha$ emission is seen, but not broad $\text{H}\beta$) and possibly some low-luminosity Seyfert 1s. Since broad emission components will preclude the use of a line-ratio diagram to discriminate between starburst and AGN galaxies (Baldwin, Phillips & Terlevich 1981), we elect to classify all 4304 galaxies by eye.

It is essential that the classification we choose is not dependent on the emission line luminosity. Since the broad and narrow emission line luminosities are strongly correlated, this requires that reddened objects where the broad emission component is near the limit of detection be included with the narrow-line objects. Objects which display broad *wings* on the $\text{H}\alpha$ line (‘Type 1.x’ galaxies) are therefore grouped with the Type 2 galaxies, while those which have clear broad $\text{H}\alpha$ and $\text{H}\beta$ emission *lines* are classified as Type 1s.

One object was discovered to have a large noise spike at the expected location of [O III] $\lambda 5007$ and was removed from the sample, since the low luminosities of the visible emission lines and the absence of the $\lambda 4959$ line indicate that its true line luminosity would be far below our lower limit.

We find that 63 objects classified as QSOs (7.1 per cent) are not QSOs at all, but display only narrow emission lines and appear to be Type 2 galaxies. We therefore reclassify them as such. We also find that 63 objects classified as galaxies (1.8 per cent) are genuinely QSOs, with clear broad line emission from both $\text{H}\alpha$ and $\text{H}\beta$, and we reclassify these objects. A further 102 (3.0 per cent) show quite pronounced broad wings on the $\text{H}\alpha$ line only, with a similar number showing weaker broad wings whose detectability

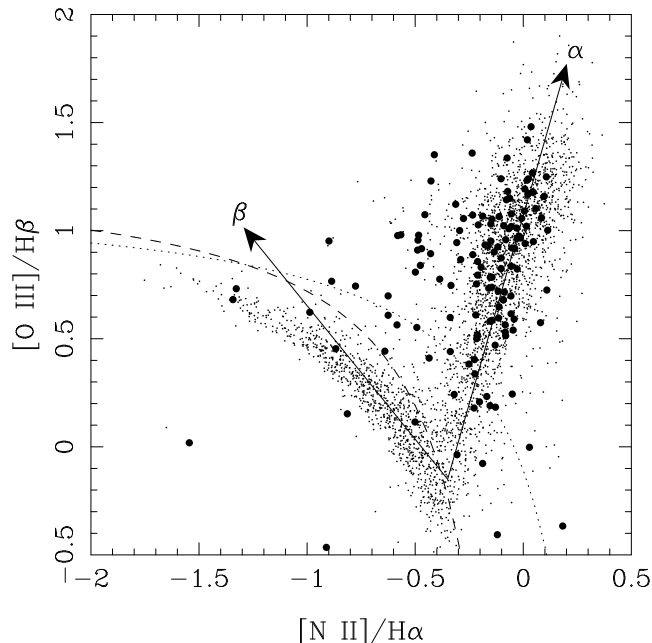


Figure 1. Emission-line ratio diagram for narrow-line objects (dots) and Type 1.x galaxies (filled circles). The α and β axes represent the ridge lines from the intersection of the AGN and starburst loci. The dotted and dashed lines are the classification criteria suggested by Kewley et al. (2001) and Kauffmann et al. (2004), respectively.

would be a function of the signal-to-noise ratio in the spectrum. A subsample of 100 objects was classified by Dr C. Done, and it was only for objects in this last category where disagreement was found. The total fraction of SDSS-classified ‘galaxies’ which we believe display broad line emission is therefore consistent with the figure of 8 per cent quoted by Kauffmann et al. (2004).

While the reason for the misclassification of Type 2 galaxies as QSOs is unclear, the Type 1s which are classified as galaxies typically have either weak broad line emission, or have very narrow permitted lines ($\sim 500 \text{ km s}^{-1}$). Our interpretation of these as *bona fide* broad-line objects is based on the presence of Fe II pseudo-continuum emission between H γ and H β , the lack of a strong 4000-Å break or Balmer jump, and a continually rising spectrum at short wavelengths.

3.2 Separation of Seyfert and starburst galaxies

We wish to construct comparable Type 1 and Type 2 samples, so that their luminosity functions (LFs) are properly representative of the population as a whole. Unfortunately, there is no straightforward way to do this. The objects we have classified as Type 1s all contain an AGN component, since the broad emission lines we observe cannot be produced by stellar processes, but they may also possess a significant contribution to their emission line luminosities from star formation activity. Objects where the line emission is almost entirely powered by star formation may not be included in this sample, however, even if we have a direct view of the broad line region, since the broad line emission will be weak. We therefore need to remove pure starburst galaxies from the sample of narrow-line objects, but also objects where the AGN contribution is so low that the objects would not have been classified as Type 1s if we had been able to see the BLR.

Kauffmann et al. (2004) use an emission-line ratio diagram

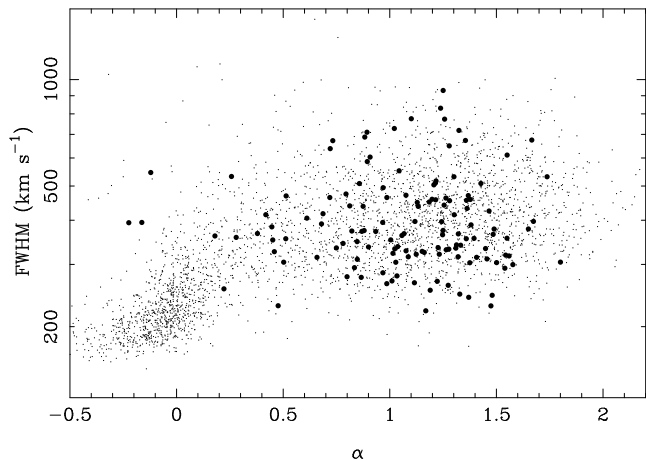


Figure 2. FWHM of the [O III] emission lines plotted against distance along the α axis of Fig. 1 for narrow-line objects (dots) and Type 1.x galaxies (filled circles).

of the type pioneered by Baldwin et al. (1981) to separate Seyferts from starburst galaxies, and we propose a similar method. Since the appropriate diagram makes use of the narrow Balmer line fluxes, it cannot be used for Type 1 AGN, where these data are unavailable. By plotting the Type 1.x galaxies on the same diagram, however, we can estimate what regions the Type 1 population would occupy. Fig. 1 displays these data.

Since our ‘Type 1.x’ classification requires that no broad H β emission is seen, the location of these points along the ordinate should be representative of the Type 1 population. Many of the Type 1.x galaxies lie in the same region as the Type 2s, because the broad H α emission is weak and the SDSS measurement therefore only includes the narrow-line flux. However, the tendency for these some of objects to have lower [N II]/H α ratios than the Type 2 population is clear, as the H α flux measurement for these includes the broad line emission. What is also clear is that some galaxies containing an AGN have low [O III]/H β ratios, and therefore any cut which excludes starburst galaxies will also exclude some *bona fide* AGN.

We attempt to find the appropriate criteria for separating Type 2 galaxies from pure starbursts by defining two (non-orthogonal) axes as shown in Fig. 1. The axes meet where the loci of the starburst and AGN sequences meet. The ‘ α ’ axis follows the ridge line of the AGN sequence, while the ‘ β ’ axis follows the ridge line of the starburst sequence. In this system, the demarcation criteria proposed by Kewley et al. (2001) and Kauffmann et al. (2004) correspond to $\alpha \approx 0.5$ and $\alpha \approx 0$, respectively.

We also consider the widths of the narrow emission lines (specifically, [O III] $\lambda 5007$) to help the differentiation between Seyfert and starburst galaxies, since it is known that the narrow lines are broader in Seyfert galaxies than in starbursts (Shuder & Osterbrock 1981). This is demonstrated to be the case in Fig. 2, where we have plotted the FWHM of the [O III] line against α as determined from Fig. 1. For the narrow-line galaxies, we have taken the value of α from their location in the (α, β) coordinate system. Since the [N II]/H α ratio for the Type 1.x galaxies is affected by broad line emission, we compute values of α for these galaxies by determining where a galaxy with the same [O III]/H β ratio would lie on the α -axis.

The overall distributions of the Type 2 and Type 1.x galaxies are inconsistent at the $\gg 99.99\%$ level, using the two-dimensional Kolmogorov–Smirnov test of Peacock (1983). However, Fig. 2

clearly shows two populations of narrow-line galaxies – a population with broad ($\text{FWHM} \gtrsim 250 \text{ km s}^{-1}$) emission lines extending to large values of α which appears to be well traced by the Type 1.x galaxies; and a population of galaxies with narrower emission lines and $\alpha \approx 0$. These two populations can be associated with Seyfert and starburst galaxies, respectively, and it is necessary to find some way to discriminate between the two classes.

Since the two distributions obviously differ greatly in the number of galaxies in the lower left corner of Fig. 2, we investigate discrimination criteria which remove these objects from the narrow-line sample. We construct a family of four-parameter selection criteria which require that α and the emission line FWHM are both greater than certain values, and also that the points satisfy the relation $\log \text{FWHM} > m(\alpha_0 - \alpha)$ where $m > 0$. We then compare the samples of narrow-line galaxies selected by each of these criteria with the complete sample of Type 1.x galaxies in the parameter space of Fig. 2, again using a two-dimensional K–S test. We find that the two distributions can be made consistent at better than 90 per cent confidence by making a simple cut with $\alpha > 0.20$. No improvement is made by imposing an additional cut based on line width, and only a very marginal gain results from adding a further selection criterion which is a function of both parameters. This selection lies approximately halfway between the criteria suggested by Kewley et al. (2001) and Kauffmann et al. (2004), as expected. The implication is that the region between their two sets of criteria represents a mixing line, with our limit being the point at which the AGN contribution becomes significant (i.e., when it is visible in the spectrum even if lightly-reddened). In the sample of 4303 emission-line galaxies there are 851 Type 1 AGN, 141 Type 1.x AGN, 2184 Type 2 AGN, and 1127 starburst galaxies (using the α criterion to classify the latter two classes).

3.3 Comparison of luminosity functions

Since the SDSS DR2 spectroscopic survey is a complete magnitude-limited survey, Type 1 galaxies will appear in relatively greater numbers because of the additional flux from the nuclear non-stellar continuum. We can however account for this by constructing LFs using the $1/V_a$ estimator (Schmidt 1968; Rowan-Robinson 1968). We then compare the Type 1 LF with the LFs of three subsamples of Type 2 galaxies, constructed by applying different selection criteria to the entire sample in an attempt to exclude the starburst galaxies. Two of these subsamples, named Type 2-Ka and Type 2-Ke, are produced by applying the line ratio selection criteria of Kauffmann et al. (2004) and Kewley et al. (2001), respectively, while the third, named Type 2- α , is constructed using the $\alpha > 0.2$ criterion derived above.

The three Type 2 LFs are compared with the Type 1 LF in Fig. 3. It is clear that, although the numbers of each type of Seyfert are similar at $L_{[\text{O III}]} \gtrsim 10^{34.5} \text{ W}$, Type 2s outnumber the Type 1s at lower luminosities by a factor of ~ 5 . Although there are differences between the numbers of lower luminosity Type 2s in the three samples, these differences are small compared to the difference between these samples and the number of Type 1s.

The different shapes of the LFs cannot be explained by a difference in the mean reddening of the Type 1 and Type 2 samples, since a reddening correction is simply a horizontal shift. The different shapes also cannot be due to problems with the Seyfert/starburst separation. The criterion defined by Kewley et al. (2001) is conservative in the sense that it should exclude *all* starburst galaxies, so the excess of Type 2 galaxies over Type 1 galaxies at lower $[\text{O III}]$ luminosities must be genuine, since even the Type 2-Ke

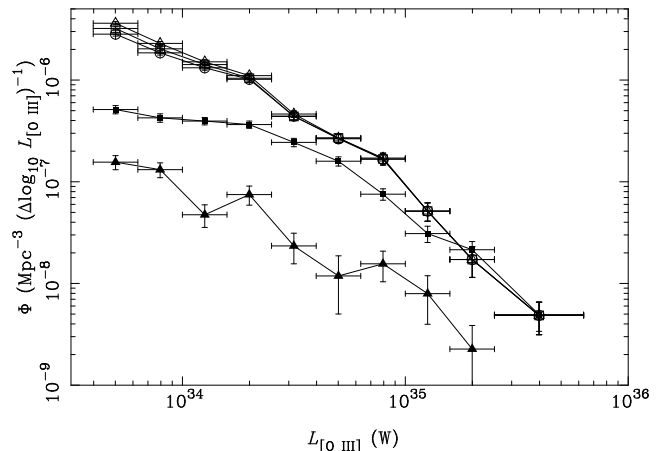


Figure 3. Luminosity functions for Type 1 galaxies (filled squares) and samples of Type 2 galaxies selected from the narrow-line objects using the criteria of Section 3.2 (open squares), Kewley et al. (2001; open circles), and Kauffmann et al. (2004; open triangles). Also shown (filled triangles) is the luminosity function of the Type 1.x galaxies, although these are also included in all the Type 2 samples.

sample exceeds the Type 1 sample. Conversely, the difference also cannot be due to an artificial deficit of high luminosity Type 2 galaxies, since all three samples have effectively the same LFs at $L_{[\text{O III}]} \gtrsim 10^{34.5} \text{ W}$.

A final possibility is perhaps that a significant fraction of the lower luminosity Type 1 galaxies have been misclassified, presumably because the broad lines are weak and below the detection threshold. This seems unlikely since the broad lines are much stronger than the narrow lines. In our Type 1 sample, the median $[\text{O III}]/\text{H}\alpha$ ratio is 0.15, while 90 per cent of objects have a ratio less than 0.5. We therefore expect all but a small fraction of Type 1 galaxies to have readily identifiable broad $\text{H}\alpha$ emission (although the $[\text{O III}]$ lines in our sample only need to be detected at $\text{S/N} > 5$, most are detected at much higher significance – all but 20 are detected at $\text{S/N} > 10$, and over half have $\text{S/N} > 20$). Furthermore, we also display the LF of the Type 1.x galaxies in Fig. 3, and there is clearly no bias against lower luminosity objects. We therefore conclude that the luminosity functions of Type 1 and Type 2 galaxies are genuinely different.

For the remainder of this paper, we use only one Type 2 luminosity function. We adopt the Type 2- α sample, and add in quadrature to the Poisson uncertainty the standard deviation of the three samples.

4 DISCUSSION

4.1 The Type 1 fraction

The different luminosity functions for our samples of Type 1 and Type 2 galaxies can also be described as a luminosity dependence of the Type 1 AGN fraction. In the context of the receding torus model, such a change is described by

$$f_1 = 1 - [1 + 3L/L_0]^{-0.5} \quad (1)$$

(e.g., Simpson 1998), where L_0 is the luminosity at which the numbers of Type 1 and Type 2 AGN are equal (i.e., an opening angle of $\theta_0 = 60^\circ$). The ‘luminosity’ of concern here is the ultraviolet–optical radiation which heats the dust, which is difficult to measure directly, but the constant equivalent width of the $[\text{O III}]$ emission

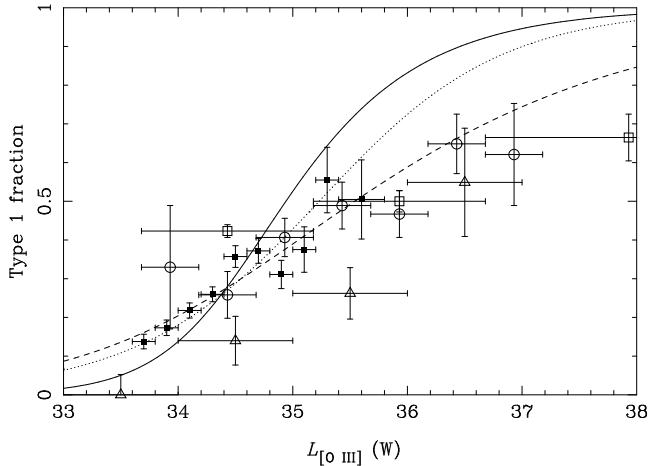


Figure 4. Type 1 AGN fraction as a function of [O III] luminosity, from this paper (solid squares), Ueda et al. (2003; open squares), Hasinger (2004; open circles), and Grimes et al. (2004; open triangles). The data from Ueda et al. and Hasinger have been converted to $L_{[\text{O III}]}$ as described in the text. The solid line shows the best-fitting ‘standard’ receding torus model (Equation 1) while the dashed line shows the best-fitting model where the torus height is allowed to vary (Equation 3), and the dotted line shows the best-fitting model where the proportionality between $L_{[\text{O III}]}$ and L_{rad} is broken (Equation 4).

line in QSOs (e.g. Miller et al. 1992; see also Simpson 1998) suggests that it should be a good tracer. Since the receding torus model is able to explain a wide range of observed AGN properties (Simpson 2003 and references therein; see also Grimes et al. 2004), we investigate whether it is also able to explain the results of the previous section.

We complement our data from similar analyses in the literature, which typically extend to higher luminosities. Both Ueda et al. (2003) and Hasinger (2004) measure the Type 1 AGN fraction in hard X-ray selected samples, which should be relatively free from orientation biases except for Compton-thick AGN, whose existence will case the Type 1 fraction to be systematically overestimated. About half of nearby low luminosity Type 2 AGN are Compton-thick (Risaliti et al. 1999) and, if this fraction is true at all luminosities then the Type 1 fraction will be overestimated by about 50 per cent. We do not make any correction for Compton-thick objects but note that the Type 1 fractions derived from X-ray-selected samples should be considered as upper limits to the true fractions. We convert the 2–10 keV luminosity (corrected for intrinsic absorption) used by these authors into [O III] luminosity using the mean ratio for Seyfert galaxies from Mulchaey et al. (1994), i.e.,

$$L_{[\text{O III}]} = 0.015 \times L_{2-10\text{keV}}. \quad (2)$$

We also add the data of Grimes et al. (2004) from the 3CRR, 6CE, and 7C flux-limited samples of radio sources. The results are shown in Fig. 4, where a clear and highly significant (> 99.99 per cent confidence) correlation between the Type 1 fraction and luminosity is seen for which the receding torus model provides an attractive, but not unique, explanation for this correlation. We note that the points from Grimes et al. (2004) tend to be slightly lower than those from the other works and this might reflect a difference in the torus properties of radio-loud and radio-quiet AGN, although the discrepancy is not highly significant.

Although the four samples plotted in Fig. 4 all show the same trend, we concentrate for now on the data from our analysis alone since there are less well understood selection effects in the X-ray

samples (see Treister et al. 2004). These cover more than two orders of magnitude in $L_{[\text{O III}]}$ but are not well-fit by the standard receding torus model, with the best fit having $\chi^2/\nu = 65.8/9$ for $L_0 = 10^{34.90}$ W.

We therefore suggest a modification to the standard receding torus model, where the height of the torus depends on the luminosity of the AGN. Such a dependence could plausibly be modulated via the mass of the black hole and the strength of its associated gravitational potential. We parametrize this dependence as $h \propto L^\xi$, and Equation 1 therefore becomes

$$f_1 = 1 - [1 + 3(L/L_0)^{1-2\xi}]^{-0.5}. \quad (3)$$

This produces a more acceptable fit ($\chi^2/\nu = 12.1/8$) for $L_0 = 10^{35.37}$ W and $\xi = 0.23$, which we also show in Fig. 4. Arshakian (2004) made a similar parametrization when studying the luminosity-dependent variations of QSO fraction and projected linear size in a radio source sample. He defined a parameter A such that $\tan \theta_c \propto L^A$ (therefore $A \equiv 0.5 - \xi$) and found $A_s = 0.35 \pm 0.09$ and $A_f = 0.26 \pm 0.02$ when considering the linear sizes and QSO fractions, respectively. The latter value is in excellent agreement with the best-fitting value of ξ we determine here.

An alternative explanation for this modification is that $L_{[\text{O III}]}$ is not a good substitute for L_{rad} , the radiative luminosity which heats the dust in the torus. If $L_{[\text{O III}]} \propto L_{\text{rad}}^{1-2\xi}$, then the standard receding torus model would fit the data. However, such an extreme disproportionality can be excluded based on a number of arguments such as the near-constancy of [O III] equivalent width in QSOs, (Miller et al. 1992), the proportionalities between [O III] luminosity and other quantities (e.g., Rawlings & Saunders 1991; Mulchaey et al. 1994; Grimes et al. 2004), and the dependence of [O III] emission on ionization parameter (Simpson 1998).

A more subtle variation in the relationship between L_{rad} and $L_{[\text{O III}]}$ may provide an explanation. In the standard unified model for AGN, only a fraction $\sim f_1$ of the ionizing radiation can escape to illuminate the narrow-line region on scales > 1 pc. This explains the (bi)conical emission-line structures seen in some Seyfert galaxies (e.g. Pogge 1989; Haniff, Wilson & Ward 1991; Simpson et al. 1997), and suggests that $L_{[\text{O III}]} \propto L_{\text{rad}} f_1$. In such a scenario,

$$f_1 = 1 - [1 + 1.5L_{[\text{O III}]} / (L_0 f_1)]^{-0.5}, \quad (4)$$

which can be rearranged to give a cubic equation in f_1 whose roots are functions of $L_{[\text{O III}]}$. This model is also shown in Fig. 4 and provides an acceptable fit (i.e. cannot be rejected at 95 per cent confidence) to our data ($\chi^2/\nu = 16.0/9$ for $L_0 = 10^{35.19}$ W).

Fig. 4 suggests that we should favour the torus described by Eqn 3 over that from Eqn 4 by virtue of the quality of fit to the X-ray datapoints. However, we caution against leaping to such a conclusion and suggest that some of the most luminous QSOs may have been misclassified as Type 2 objects. While this seems counterintuitive, such objects will inevitably be at the highest redshifts and therefore the optical spectroscopy performed on them will sample the rest-frame ultraviolet. Even relatively small amounts of dust could be sufficient to extinguish the broad emission lines and give such objects the appearance of a Type 2 AGN in the UV. While there should be very few luminous AGN which are lightly reddened because the observer’s line of sight just grazes the torus (see Hill et al. 1996), the required extinctions may arise from dust in the host galaxy which is not associated with the active nucleus. The repeated reclassifications of ‘Type 2 QSOs’ after near-infrared spectroscopy reveals broad H α emission (e.g., Halpern, Eracleous & Forster 1998; Halpern, Turner & George 1999; Akiyama, Ueda &

Ohta 2002) suggests that there may be some truth in this. On the other hand, the QSO fraction may be overestimated if there exists a significant population of luminous AGN with Compton-thick tori which are not detected in hard X-ray surveys. What is required is a systematic near-infrared study of either spectroscopy or imaging, similar to that which Simpson et al. (1999) performed for $z \sim 1$ powerful radio sources. This should be possible in the very near future with the combination of *Chandra* or *XMM-Newton* and *Spitzer* imaging in a number of fields.

Having suggested that both modifications to the receding torus model fit the data equally well, we return to the issue of whether breaking the proportionality between the ionizing and [O III] emission-line luminosities is in conflict with observations. First, this does not affect the isotropy of the [O III] emission, since the emission-line luminosities of Type 1 and Type 2 AGN with similar ionizing luminosities should still be the same. However, it predicts that the observed equivalent width of [O III] should be proportional to f_1 (i.e., increase with increasing AGN luminosity), whereas observations show it to be constant with luminosity (Miller et al. 1992). However, over the range of luminosities studied by Miller et al. (approximately two orders of magnitude), f_1 is predicted to vary by a factor of about 2, which is equal to the 1σ scatter in the rest-frame equivalent width. Furthermore, this effect will be lessened by those objects seen at small polar angles where the continuum, but not the emission-line, luminosity is enhanced. A quantitative analysis of this effect depends on the assumed angular and wavelength dependence of the ionizing continuum and is therefore rather model-dependent and beyond the scope of this paper. However, we do predict that the scatter in the equivalent width of the [O III] line should increase with luminosity.

4.2 Implications for AGN evolution

Studies of AGN evolution have so far primarily relied on samples of QSOs since these objects are readily visible out to large distances. Obviously such samples contain only a fraction of the AGN at any redshift or luminosity since Type 2 objects do not meet the colour and/or morphological selection criteria (while hard X-ray surveys are less biased against Type 2 AGN, they presently lack the combination of depth and area coverage to properly sample the AGN luminosity function in an unbiased manner). We therefore wish to determine how the luminosity-dependent QSO fraction might affect the conclusions drawn from studies of QSO evolution.

Since there is a significant stellar component to the broad-band magnitudes of our Type 1 galaxies which is not the case for observed samples of QSOs, we estimate the non-stellar continuum luminosities from our [O III] luminosities. We assume a mean rest-frame equivalent width (relative to the non-stellar continuum) for the $\lambda 5007$ line of $\epsilon = 24 \text{ \AA}$ (Miller et al. 1992), and a spectral shape $S_\nu \propto \nu^{-0.44}$ (Vanden Berk et al. 2001; the result is extremely insensitive to the shape of the spectrum due to the small wavelength difference between the [O III] line and the B band) in the rest-frame optical. It then follows that

$$M_B = -22.0 - 2.5 \log(L_{[\text{O III}]} / 10^{35} \text{ W}) + 2.5 \log(\epsilon / 24 \text{ \AA}) \quad (5)$$

and $M_{b_J} = M_B - 0.09$ for the canonical QSO spectrum (Blair & Gilmore 1982).

Our Type 1 LF can be well-fit with the two power-law parametrization of the 2QZ team,

$$\Phi(L) = \frac{2\Phi(L^*)}{(L/L^*)^{-\alpha} + (L/L^*)^{-\beta}} \quad (6)$$

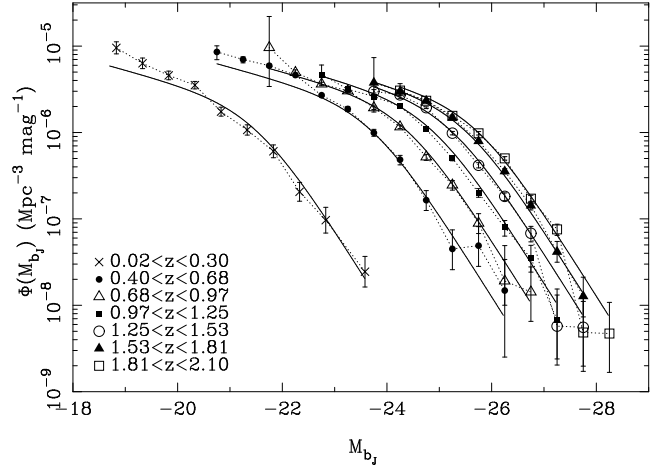


Figure 5. Our Seyfert (Types 1 and 2) luminosity function converted to M_{b_J} (crosses) and plotted with the modified QSO optical luminosity functions of Croom et al. (2004; all other symbols). A two power-law model with pure luminosity evolution has been fitted to the data, as described in the text, and the results are shown by the solid curves.

(e.g., Croom et al. 2004; note that the normalization factor of 2 is missing from papers by this team). A good fit ($\chi^2/\nu = 4.8/6$) is found with the parameters $\alpha = -2.86$, $\beta = -1.06$, $L^* = 3.5 \times 10^{34} \text{ W}$, and $\Phi^* = 2.24 \times 10^{-7} \text{ Mpc}^{-3} \text{ dex}^{-1}$. The power law indices are similar to those derived by Croom et al. (2004), who found $\alpha = -3.25$ and $\beta = -1.01$. However, a better comparison would be to the combined (i.e., Types 1 and 2) Seyfert LF since, while the Croom et al. (2004) LFs are relatively insensitive to the lack of Type 2 objects, our Type 1 LF is a poor representation of the overall AGN LF. The fit to the combined Seyfert luminosity function is improved ($\chi^2/\nu = 3.3/6$), primarily due to the larger error bars resulting from the uncertain classification of narrow-line objects, with $\alpha = -3.11$, $\beta = -1.59$, $L^* = 4.4 \times 10^{34} \text{ W}$, and $\Phi^* = 5.25 \times 10^{-7} \text{ Mpc}^{-3} \text{ dex}^{-1}$.

There is moderately good agreement between the values of M^* and Φ^* from our combined Seyfert sample and the extrapolation of the exponential pure luminosity evolution of Croom et al. (2004). We obtain $M_{b_J}^* = -21.20$ and $\Phi^* = 1.31 \times 10^{-6} \text{ Mpc}^{-3} \text{ mag}^{-1}$ compared to $M_{b_J}^* = -21.46$ and $\Phi^* = 1.84 \times 10^{-6} \text{ Mpc}^{-3} \text{ mag}^{-1}$ from their work (the agreement is less good for the polynomial evolution, where a value of $M_{b_J}^* = -22.15$ is predicted for our sample). The lower space density we derive cannot be due to incompleteness in our sample of Seyfert galaxies since our spectroscopic selection will include all such objects (accounting for the uncertainty in the starburst–Seyfert classification), whereas the optical colour selection used to select QSOs will exclude a population of red QSOs which may exist in significant numbers (Webster et al. 1995; Benn et al. 1998; Richards et al. 2003).

We also try to simultaneously fit our Seyfert LF and the six QSO LFs of Croom et al. (2004), after using the modified receding torus model to account for the missing Type 2 objects. We use their two power-law model with an exponential form for the luminosity evolution, although we fit the value of M^* for our Seyfert LF as a separate parameter since an extremely poor fit is obtained otherwise. Following Croom et al., we use only the $M_{b_J} < -22.5$ bins, and we show the best fit in Fig. 5. While this fit is unacceptably poor in a formal sense ($\chi^2/\nu = 175/58$), it does reproduce the gross characteristics of the evolving LF and, in particular, the

power law indices differ from those derived from the Type 1 (QSO) LF alone.

Unsurprisingly, the value of α is least affected. From our earlier calculation that $L_0 = 10^{35.53}$ W, we conclude that QSOs outnumber Type 2 objects where $M_B \lesssim -23.3$ and therefore the bright end of the luminosity function is not strongly affected by the absence of Type 2 objects and the power law slope is only moderately steepened by their inclusion – we find $\alpha = -3.42$ as opposed to $\alpha = -3.25$. However, the faint end slope is made much steeper ($\beta = -1.41$ compared to $\beta = -1.01$), and is closer to the faint-end slope of the hard X-ray luminosity function ($\beta = -1.86$; Ueda et al. 2003). This steepening has a large effect on the contribution from faint AGN to the overall AGN luminosity. Integrating the two power-law model, the total luminosity from AGN with $L > L^*$ is $\sim 0.4\Phi^*L^*$. The total luminosity from AGN fainter than L^* does not converge for $\beta < -1$ and so is dependent on the low-luminosity cutoff, but in the decade below L^* , it is $\sim 2.3\Phi^*L^*$ for $\beta \approx -1.0$ and nearly twice as much for $\beta \approx -1.5$. Wolf et al. (2003) find a downturn in the shape of the LF at faint absolute magnitudes ($M_B > -22$, not probed by 2QZ) which allows the luminosity density integral to converge. However, the increased number of Type 2 AGN predicted at these luminosities significantly affects the strength of this downturn and therefore the contribution by faint AGN to the overall luminosity density. Such objects would be fainter than the low-luminosity Type 1 AGN studied by Wolf et al. (2003) and therefore could not have yet been spectroscopically identified in deep X-ray surveys such as Barger et al. (2003). Given that a putative further population of Compton-thick Type 2 AGN would not even appear in such X-ray surveys, there is a distinct likelihood that the importance of low luminosity AGN has been significantly underestimated.

Finally, while attempting to tie the present-day black hole mass density to the evolution of QSOs, Yu & Tremaine (2002) note that their results are dependent on the prevalence of obscured low-luminosity AGN. In particular, the accretion efficiency can be made roughly independent of AGN luminosity if the obscured AGN fraction is larger for low mass black holes, and hence less luminous AGN, as predicted by the receding torus model.

4.3 The Cosmic X-ray Background

While the predictions of the receding torus model agree well with the observed number of X-ray-selected Type 2 AGN, models for the CXB (e.g., Comastri et al. 1995; Wilman, Fabian & Nulsen 2000) require the presence of an additional Compton-thick population which is not detectable in such surveys. As discussed previously, this means the true Type 1 fraction is lower than the observations suggests, and hence there is an apparent discrepancy between the receding torus model and models for the CXB.

However, the number of Compton-thick AGN proposed is a relatively small fraction of the total AGN population. Ueda et al. (2003) fit the CXB by proposing that there are as many AGN with $10^{24} \text{ cm}^{-3} < N_H < 10^{25} \text{ cm}^{-3}$ as with $10^{23} \text{ cm}^{-3} < N_H < 10^{24} \text{ cm}^{-3}$, but there is a strong luminosity dependence in the shape of the N_H distribution. Therefore, while there are many Compton-thick AGN at low redshift/luminosity (Risaliti et al. 1999), there are many fewer at the redshift/luminosity which produces the bulk of the CXB.

In addition, Type 1 AGN with significant X-ray obscuration are known to exist, the original member of this class being MR 2251–178 (Halpern 1984; see also Page et al. 2004), so the Type 1 fraction need not be the same as the fraction of X-ray unab-

sorbed AGN. Although the column densities of these objects tend not to exceed $\sim 10^{22.5} \text{ cm}^{-2}$, Willott et al. (2003, 2004) have found objects with greater absorption ($N_H > 10^{23} \text{ cm}^{-2}$) whose optical/infrared spectra are consistent with lightly-reddened QSOs. It is therefore possible that the most heavily absorbed AGN also suffer significant non-torus reddening and may have escaped detection in both X-ray and optical QSO surveys.

Finally, a large discrepancy between the receding torus model and the observations of hard X-ray-selected AGN occurs only at very high luminosities ($L_{\text{[OIII]}} > 10^{36}$ W, or $L_X > 10^{38}$ W) and this population contributes almost negligibly to the overall CXB (e.g., figs 16 and 17 of Ueda et al. 2003). We conclude therefore that the receding torus model does not conflict with our current understanding of the Cosmic X-ray Background.

5 SUMMARY

We have constructed separate luminosity functions for Seyfert 1 and Seyfert 2 galaxies, using the Second Data Release of the Sloan Digital Sky Survey. We have shown that these luminosity functions have different shapes, resulting in an increase in the Type 1 AGN fraction with luminosity which is in quantitative agreement with that determined from hard X-ray-selected samples. We show that the form of this luminosity dependence is inconsistent with the standard receding torus model, and propose a modification where the height of the torus varies with luminosity as $h \propto L^{0.26}$, although we note that a more robust spectral classification of distant luminous AGN is desired. Assuming that this modification to the receding torus model provides a reasonable correction factor to account for the ‘missing’ Type 2 AGN in QSO surveys, we have shown that the contribution to the cosmic accretion luminosity from faint AGN may have been significantly underestimated.

ACKNOWLEDGMENTS

I would like to thank Matt Jarvis for useful discussions, Chris Done for agreeing to classify a subsample of spectra, and the referee, Andy Lawrence, for his helpful report. I also wish to thank PPARC for financial support in the form of an Advanced Fellowship.

Funding for the creation and distribution of the SDSS Archive has been provided by the Alfred P. Sloan Foundation, the Participating Institutions, the National Aeronautics and Space Administration, the National Science Foundation, the U.S. Department of Energy, the Japanese Monbukagakusho, and the Max Planck Society. The SDSS Web site is <http://www.sdss.org/>.

The SDSS is managed by the Astrophysical Research Consortium (ARC) for the Participating Institutions. The Participating Institutions are The University of Chicago, Fermilab, the Institute for Advanced Study, the Japan Participation Group, The Johns Hopkins University, Los Alamos National Laboratory, the Max-Planck-Institute for Astronomy (MPIA), the Max-Planck-Institute for Astrophysics (MPA), New Mexico State University, University of Pittsburgh, Princeton University, the United States Naval Observatory, and the University of Washington.

REFERENCES

- Akiyama M., Ueda Y., Ohta K., 2002, *ApJ*, 567, 42
- Antonucci R., 1993, *ARA&A*, 31, 473
- Arshakian T. G., 2004, *A&A*, submitted (astro-ph/0411636)

- Baldwin J. A., Phillips M. M., Terlevich R., 1981, *PASP*, 93, 5
- Barger A. J., et al., 2003, *AJ*, 126, 632
- Benn C. R., Vigotti M., Carballo R., Gonzalez-Serrano J. I., Sánchez S. F., 1998, *MNRAS*, 295, 451
- Benson A. J., Bower R. G., Frenk C. S., Lacey C. G., Baugh C. M., Cole S., 2003, *ApJ*, 599, 38
- Blair M., Gilmore G., 1982, *PASP*, 94, 742
- Clavel J., Wamsteker W., Glass I. S., 1989, *ApJ*, 337, 236
- Cole S., Lacey C. G., Baugh C. M., Frenk C. S., 2000, *MNRAS*, 319, 168
- Comastri A., Setti G., Zamorani G., Hasinger G., 1995, *A&A*, 296, 1
- Croom S. M., Smith R. J., Boyle B. J., Shanks T., Miller L., Outram P. J., Loaring N. S., 2004, *MNRAS*, 349, 1397
- Dahari O., De Robertis M. M., 1988, *ApJ*, 331, 727
- Elvis M., et al., 1994, *ApJS*, 95, 1
- Fabian A. C., 1999, *MNRAS*, 308, L39
- Grimes J. A., Rawlings S., Willott C. J., 2004, *MNRAS*, 349, 503
- Halpern J. P., 1984, *ApJ*, 281, 90
- Halpern J. P., Eracleous M., Forster K., 1998, *ApJ*, 501, 103
- Halpern J. P., Turner T. J., George I. M., 1999, *MNRAS*, 307, L47
- Haniff C. A., Wilson A. S., Ward M. J., 1991, *ApJ*, 368, 168
- Hasinger G., 2004, *Nucl. Phys. B Proc. Supp.*, 132, 86
- Hill G. J., Goodrich R. W., DePoy D. L., 1996, *ApJ*, 462, 163
- Kauffmann G., Haehnelt M., 2000, *MNRAS*, 311, 576
- Kauffmann G., et al., 2003, *MNRAS*, 346, 1055
- Kewley L. J., Dopita M. A., Sutherland R. S., Heisler C. A., Trevena J., 2001, *ApJ*, 556, 121
- Kobayashi Y., Sato S., Yamashita T., Shiba H., Takami H., 1993, *ApJ*, 404, 94
- Lawrence A., 1991, *MNRAS*, 252, 586
- McLure R. J., Dunlop J. S., 2002, *MNRAS*, 331, 795
- Miller P., Rawlings S., Saunders R., Eales S., 1992, *MNRAS*, 254, 93
- Mulchaey J. S., Koratkar A., Ward M. J., Wilson A. S., Whittle M., Antonucci R. R. J., Kinney A. L., Hurt T., 1994, *ApJ*, 436, 586
- Page M. J., Stevens J. A., Ivison R. J., Carrera F. J., 2004, *ApJ*, 611, L85
- Peacock J. A., 1983, *MNRAS*, 202, 615
- Pogge R. W., 1989, *ApJ*, 345, 730
- Rawlings S., Saunders R., 1991, *Nat*, 349, 138
- Richards G. T., et al., 2003, *AJ*, 126, 1131
- Risaliti G., Maiolino R., Salvati M., 1999, *ApJ*, 522, 157
- Rowan-Robinson M., 1968, *MNRAS*, 138, 445
- Schmidt M., 1968, *ApJ*, 151, 393
- Schmidt M., Green R. F., 1983, *ApJ*, 269, 352
- Shuder J. M., Osterbrock D. E., 1981, *ApJ*, 250, 55
- Silk J., Rees M. J., 1998, *A&A*, 338, 1
- Simpson C., 1998, *MNRAS*, 297, L39
- Simpson C., 2003, *NewAR*, 47, 211
- Simpson C., Rawlings S., 2000, *MNRAS*, 317, 1023
- Simpson C., Rawlings S., Lacy M., 1999, *MNRAS*, 306, 828
- Simpson C., Wilson A. S., Bower G. A., Heckman T. M., Krolik J. H., Miley G. K., 1997, *ApJ*, 474, 121
- Treister E., et al., 2004, *ApJ*, in press (astro-ph/0408099)
- Ueda Y., Akiyama M., Ohta K., Miyaji T., 2003, *ApJ*, 598, 210
- Vanden Berk D. E., et al., 2001, *AJ*, 122, 549
- Wake D. A., et al., 2004, *ApJ*, 610, L85
- Webster R. L., Francis P. J., Peterson B. A., Drinkwater M. J., Masci F. J., 1995, *Nat*, 375, 469
- Willott C. J., Rawlings S., Blundell K. M., Lacy M., 2000, *MNRAS*, 316, 449
- Willott C. J., et al., 2003, *MNRAS*, 339, 397
- Willott C. J., et al., 2004, *ApJ*, 610, 140
- Wilman R. J., Fabian A. C., Nulsen P. E. J., 2000, *MNRAS*, 319, 583
- Wilson A. S., Tsvetanov Z. I., 1994, *AJ*, 107, 1227
- Wolf C., Wisotzki L., Borch A., Dye S., Kleinheinrich M., Meisenheimer K., 2003, *A&A*, 408, 499
- York D. G., et al., 2000, *AJ*, 120, 1579
- Yu Q., Tremaine S., 2002, *MNRAS*, 335, 965